Titania Supported Tungsten Oxide Species Studied by Raman Spectroscopy

Sang Hoon Han, Hack Sung Kim, and Kwan Kim*

Department of Chemistry, College of Natural Sciences, Seoul National University, Seoul 151-742
Receiveel September 10, 1990

Laser Raman spectroscopy has been used to study the tungsta catalyst supported on titania. The surface tungsten species which forms on titania after calcination appeared to possess a structure that is independent of the initial impregnation condition. The surface polytungstate seemed to be stable only at the interfacial region since the crystalline WO_3 phase was observed as long as the tungsta loading was in excess of monolayer coverage. The close intact and strong interaction between the polytungstate and the titania could be evidenced from the inhibition of the phase transition of TiO_2 from anatase to rutile.

Introduction

Supported oxides of transition metals of group VIb are widely used as catalysts for various reactions. For example, alumina supported molybdenum based catalysts are extensively used in the hydrotreating processes such as hydrodesulfurization, hydrodenitrogenation and hydrodemetalization of petroleum or coal products[1-5]. A number of studies on the characterization of the catalysts have thus been made in the past decade. Most of the works are, however, concerned with the characterization and the catalytic performance of alumina supported systems[6-9]. The titania supported catalysts have attracted much less attention. One reason is that the catalytic activity was considered to be much lower compared with the alumina-supported catalysts. Nevertheless, titania-supported molybdenum catalysts are reported recently to be active for a wide range of important reactions such as olefin hydrogenation and isomerization[10].

There is considerable current interest in the strong interaction between certain oxide support and metal phase (SMSI)[11-13]. In addition, the interaction between oxide supports and highly dispersed oxide phases is receiving increasing attention[14-17]. Titania is a typical SMSI oxide. Accordingly, one may expect that titania would modify the surface state of the supported molybdena or tungsta. We have recently applied the FT-IR[18] and the laser Raman[19] spectroscopies to the characterization of the titania supported molybdena catalyst. In the present work, we have performed the Raman spectroscopic study on the titania-supported tungsta system. Raman spectroscopy is very effective in detecting the presence of the crystalline as well as amorphous oxides[20].

To our knowledge, Raman spectroscopic study on titania-supported tungsta catalysts is scarce and little is know about the structure of surface species[19]. Chan *et al*[21]. reported the Raman spectral feature for a sample containing 7 wt% WO_3 in titania after calcination at 773 K in dry air. On the other hand, Wachs and Hardcastle[22] reported the Raman specturm of 5 wt% tungsten oxide on titania calcined at 773 K in the normal air. According to the recent X-ray absorption near-edge spectroscopy studies[23] on 5 wt% WO_3/Al_2O_3 sample, the coordinatively unsaturated tungsta species seems not to form upon calcination in wet air.

The purpose of this work is to know further the structural nature of the titania-supported tungsten oxide phase. It is intended in the present work to provide the following informations; (i) effect of the sample preparation condition (pH) on the surface tungsten species, (ii) dependence of the formation of surface species on the calcination temperature and the % loading, (iii) effect of the incorporation of additives such as Ni and Co on the structure of surface tungsten species, (iv) spreading and reaction of WO_3 on the titania surface, (v) stability of the surface tungsten species, (vi) extent of interaction between the titania and the surface tungsten species. Since we are, at the moment, interested in the coordinatively saturated surface tungsten species, the calcination treatment has been performed in air.

Experimental

The tungsten oxide on titania (Degussa, P-25, 50 m^2/g) samples were prepared by the incipient wetness impregnation method by adding an aqueous solution of ammonium paratungstate to the titania powder. The solution pH was adjusted to the desired value by either HNO_3 or NH_4OH. The wet catalysts were dried in air at 373 K for 72 hrs. Then, the thoroughly ground samples were calcined in air at 673, 823, or 973 K for 16 hrs. To prepare the samples containing promoters, the co-impregnation method was employed with a cobalt or nickel nitrate solution. After calcination, some samples have been reduced under flowing hydrogen at 673 K for 16 hrs. Besides, some samples were prepared by the physical mixing method. The WO_3 was obtained by thermal decomposition of ammonium paratungstate in air at 773 K for 8 hrs. The formation of WO_3 was confirmed by the X-ray diffraction analysis. After a thorough grinding, the mixtures of WO_3 and TiO_2 have been pelletized and then subjected to calcination. All the chemicals used in this work were reagent grade, and triply distilled water was used in the preparation of aqueous solutions.

Raman spectra were obtained with a Japan spectroscopic Model R-300 laser Ramen spectrometer. The 514.5 nm line from a Spectra Physics Model 164-06 argon ion laser was used as the exciting source. Raman scattering was observed at 90° geometry with a commercial photon counting system. The typical laser power was 20-40 mW at the sample position. The pelletized sample was spun at 2000 rpm during

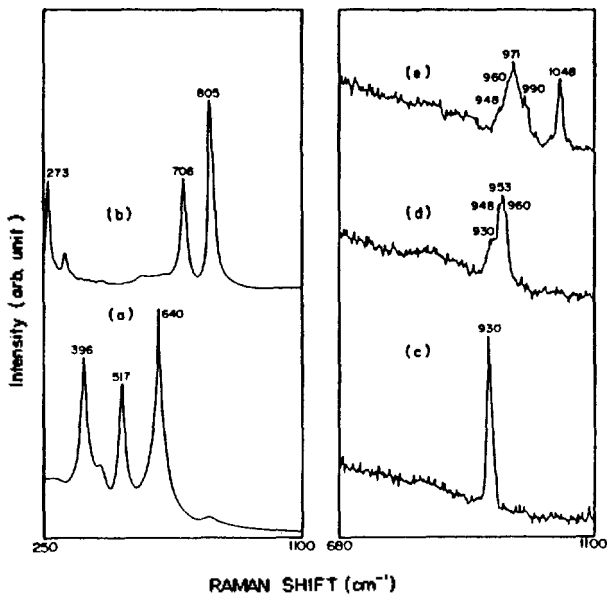

Figure 1. Raman spectra of reference compounds; (a) TiO_2 (b) WO_3 and tungstate solutions at pH 11.5 (c) 6.8 (d) and 2 (e).

the Ramam measurement to reduce the local heating from the continuous laser radiation. All the spectra were obtained at room temperature and under ambient conditions.

Results and Discussion

In order to facilitate the interpretation of the Raman spectra of tungsta catalysts, spectra of various reference compounds have been recored. Figure 1a represents the Ramam spectrum of titania support. The major anatase bands occur at 396, 517, and 640 cm $^{-1}$, while the bands due to rutile at 448 and 611 cm $^{-1}$. It is seen that the spectrum is dominated by the anatase feature. As shown in Figure 1b, WO_3 can be characterized by the prominent peaks at 805, 706, and 273 cm $^{-1}$, where 805 and 706 cm $^{-1}$ are assingned as W-O-W stretching frequencies and 273 cm $^{-1}$ as a W-O-W bending mode[24]. Figure 1c, 1d, and 1e exhibit, respectively, the Raman spectra of tungstate solutions at pH 11.5, 6.8 and 2. In Figure 1c, there is a sharp peak at 930 cm $^{-1}$ (W=O stretch) and a broad peak at 834 cm $^{-1}$(W-O-W asymmetric stretch) characteristic of the monomeric WO_4^{2-} anion[25]. As the pH is lowered to 6.8 aggregation starts and a new peak appears at 953 cm $^{-1}$. It is known that the paratungstate-A ion, $HW_6O_{21}^{5-}$, forms at a pH of 5-6 by the reaction[25]

$$6WO_4^{2-} + 7H^+ \rightleftharpoons HW_6O_{21}^{5-} + 3H_2O$$

The paratungstate-A ion is in slow equilibrium with the paratungstate-B ion, $W_{12}O_{36}(OH)_6^{6-}$,

$$2W_6O_{20}(OH)^{5-} + 4H_2O \rightleftharpoons W_{12}O_{36}(OH)_{10}^{10-}$$

At high concentrations, the B ion is known to be predominant[26]. The peak at 953 cm $^{-1}$ in Figure 1d is due to the polymeric tungstate species, mostly likely the paratungstate-A anion. As the pH is decreased to 2, the 930 cm^{-1} band is completely absent and a peak centered at 971 cm^{-1} appears along with shoulder peaks at 990 and 948 cm^{-1} as can be seen from Figure 1e. The 971 cm^{-1} peak is supposed to arise from the paratungstate-B species. The identity of the shoulder peak at 990 cm^{-1} is, however, rather uncertain[26].

Tetrahedrally coordinated molecules of the type WO_4 possess four fundamental vibrational modes, $\nu_1(A_1)+\nu_2(E)+\nu_3(F_2)+\nu_4(F_2)$, and all are Raman active[27]. The tungstate ion in aqueous solution, WO_4^{2-}, has an ideal tetrahedral structure and the four fundamental modes are observed, as mentioned above, at 930 (A_1), 324 (E), 834 (F_2), and 324 cm $^{-1}$ (F_2). Crystalline Na_2WO_4 has a spinel structure with tetrahedral site symmetry[28], and its four modes are observed at 928 (A_1), 312 (E), 813 (F_2), and 373 cm $^{-1}$ (F_2). Crystalline $CaWO_4$ has a scheelite structure[29] where the WO_4 group is slightly distorted from the ideal tetrahedron with the site symmetry of S_4. The Raman modes split due to this distortion, and $CaWO_4$ Ramam bands[23] are found at 922, 838, 794, 403, 334, 210, and 118 cm $^{-1}$.

Octahedrally coordinated molecules of type WO_6 possess only three Raman-active modes[27], $\nu_1(A_{1g})+\nu_2(E_g)+\nu_5(F_{2g})$. One of the ideal WO_6 octahedron is known to be crystalline Li_6WO_6, and its three fundamental modes[30] occur at 740 (A_{1g}), 430 (E_g), and 360 cm^{-1} (F_{2g}). Crystalline WO_3 possesses the cubic ReO_3 structure, the simplest three-dimensional structure formed from vertex-sharing octahedral groups, and its major Raman bands occur, as mentioned earlier, at 805, 706, and 273 cm^{-1}. The crystalline $CoWO_4$ and $NiWO_4$ have octahedral coordinations, and their highest wavenumber Raman bands appear at 886 and 893 cm^{-1}, respectively. The position of the highest Raman band is generally known to reflect the highest bond order (shortest W-O band) present in the tungsten oxide structure[24,31]. Hence, as can be noticed from the above discussions, regular tetrahedral WO_4 groups exhibit, in general, Raman bands at higher wavenumber than regular octahedral WO_6 groups because of their higher bond order (shorter W-O bond). Distortions in the tetrahedral WO_4 and octahedral WO_6 groups, however, can give rise to very significant increases in the W-O bond order of both structures. For instance, ammonium metatungstate, $(NH_4)_6H_2(W_3O_{10})_4$, possesses WO_6 octahedra of significant distortion, and the symmetric stretch appears at about 980 cm $^{-1}$. Similarly, as can be seen from Figure 1e, the polymeric tungstate species exhibit a strong peak at 971 cm^{-1}. Hence, it appears difficult to adequately differentiate between tungsten oxide tetrahedral and octahedral species by using the symmetric stretch as a rough guideline.

Raman spectra of tungsta on titania samples recorded for the two stages, *i.e.*, dried at 373 K and calcined at 823 K, during their preparation are shown in Figure 2 in a limited region, 800-1100 cm $^{-1}$. The samples contain 6.2 wt% WO_3, which is less than that required to achieve a complete monolayer coverage, and were impregnated initially at pH 11.5, 6.8, and 2. In the dried state, a relatively broad and asymmetric feature appeared at 950 cm $^{-1}$ for both samples impregnated at basic and neutral pH's (see Figure 2a and 2b). On the other hand, the sample impregnated at acidic pH exhibited a similar band at 966 cm^{-1}, as can be seen from Figure 2c (the 1048 cm^{-1} peak is due to NO_3^-). The corresponding band usually shows some structure or splitting in the wet state of the samples which is lost during the drying procedure[32]. According to Ng and Gulari[25], in a 0.1 M tungstate solution at pH 7.3, 16% of the tungstate is in polymeric form, while 80% is in the polymeric form at pH 4.9. Hence, the

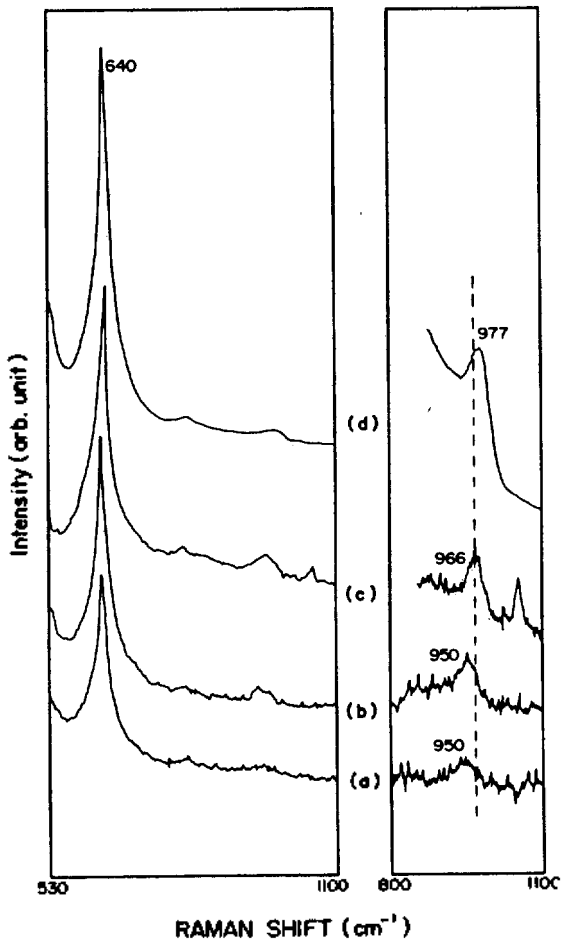

Figure 2. Raman spectra of 6.2 wt% WO_3 on TiO_2 in the dried and calcined states. (a), (b), and (c) were recorded after drying at 373 K for the samples prepared initially at pH 11.5 (a), 6.8 (b) and 2 (c), respectively. (d) was uniquely obtained after calcining at 823 K regardless of the initial impregnation condition.

peak at 950 cm^{-1} in Figure 2a and 2b can be attributed, mainly, to the adsorb WO_4^{2-} ions. The peak at 966 cm^{-1} in Figure 2c should be due to the polymeric tungstate species, most likely the paratungstate-B. Nevertheless, it is interesting to observe that after calcination at 823 K all three samples possess the same spectral feature. Neither the formation of WO_3 nor the phase transition of TiO_2 has taken place. One prominent peak appeared at 977 cm^{-1} irrespective of the impregnation condition (see Figure 2d). As argued in the earlier discussion, it is rather difficult, however, to distinguish whether the tungsten oxide surface species is octahedrally or tetrahedrally coordinated to the titania support.

Recently, Horsley *et al.*[23] applied the X-ray absorption near-edge spectroscopy (XANES) to the characterization of WO_3/γ-Al_2O_3 system. When the sample with submonolayer coverage was calcinced at 773 K, in the absence of coordinated water, the XANES spectrum indicated a distorted tetrahedral structure for the surface tungsten oxide species. Samples exposed to air at room temperature was reported, however, to have water molecules coordinated to some fraction of the sites, producing an octahedral site symmetry. On the other hand, at high coverage a significant fraction of the

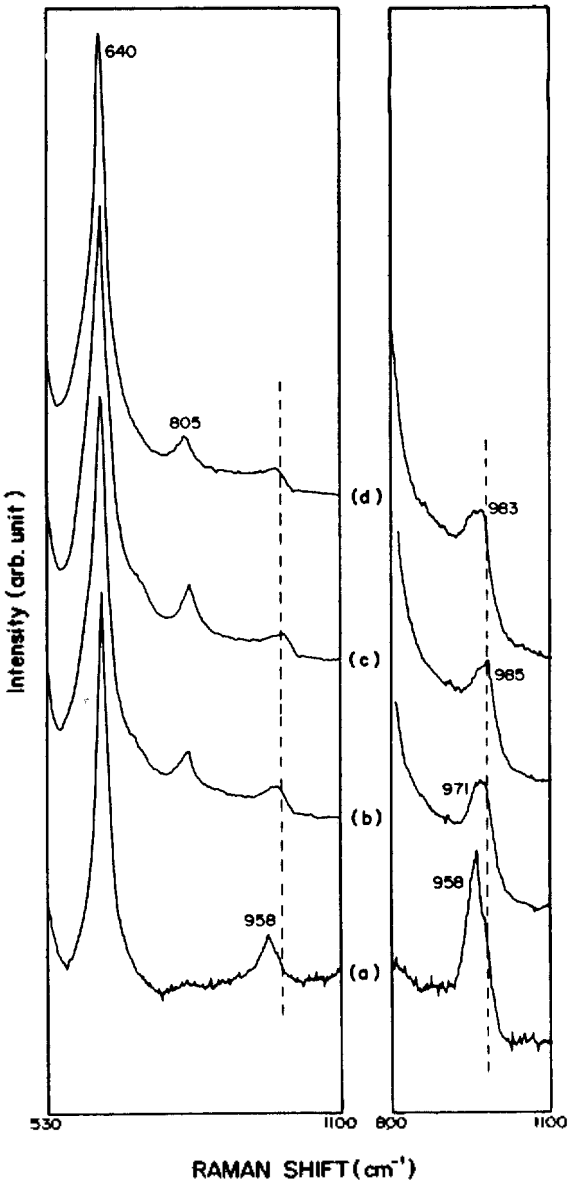

Figure 3. Raman spectra of 10.2 wt% WO_3 on TiO_2, prepared initially at pH 6.8, after drying at 373 K (a) and calcining at 673 (b), 823 (c) and 973 K (d).

surface tungsten sites seemed to possess a distorted octahedral environment even after dehydration by heating to 773 K. Based on this report, we propose that the tungsten surface species responisible for Figure 2d has an octahedral structure since the samples in the present work have been calcined in air and the Raman spectra have been taken under the ambient condition. From the fact that in the dried state the Raman spectral feature of the sample prepared at the acidic medium is different from that of the sample impregnated at the basic environment, but much the same as each other after calcination, it can be conjectured that the formation of octahedral surface tungstate is a favorable process during calcination in air, regardless of the structure in the dried state. Since the peak position observed after calcination (977 cm^{-1}) is nearly the same as that (971 cm^{-1}) observed for the solution used in the impregnation at acidic pH, the

surface tungstate is supposed further to have a structure similar to paratungstate. Hence, we may call the tungsten species on titania "surface polytungstate".

Figure 3 shows the Raman spectra for the system containing 10.2 wt% WO_3 in TiO_2 after calcination at different temperatures. The sample was initially impregnated at pH 6.8. In the dired state the band due to surface tungsten species appeared at 958 cm^{-1} as can be seen in Figure 3a. The corresponding band occurred at 939 and 950 cm^{-1}, respectively, for the sample containing 2.5 and 6.2 wt% WO_3. Hence, the band shifted to higher frequencies as the tungsta loading increased. This may indicate that the surface species with tetrahedral site symmetry assumes a more distorted structure at higher surface concentration. As the sample was calcined at 673, 823, and 973 K, the peak attributable to surface polytungstate species appeared at 971, 985, and 983 cm^{-1}, respectively. As the calcination temperature increases, the band is observed to become broadened. This may indicate that the octahedral surface species possesses a more distorted characteristics at higher thermal treatment. On the other hand, the formation of WO_3 phase is evidenced following the calcination process (see the 805 cm^{-1} peak in Figure 3). Such a phase could not be detected, however, for the sample containing 6.2 wt% WO_3 in TiO_2. This means that the 10.2 wt% sample contains tungsta in excess of monolayer coverage on titaina. When the sample containing 6.2 wt% WO_3 in TiO_2 was calcined at 673, 823, and 973 K, the peak due to surface tungsten species appeared at 970, 975, and 974 cm^{-1}, respectively. For the case of the sample with 2.5 wt% WO_3, the corresponding peak was observed at near 952 cm^{-1}, irrespective of the calcination temperature. Therefore, it appears that the surface species in the sample with 6.2 wt% WO_3 is somewhat different from that in the sample with 2.5 wt% WO_3. Considering that the peak position (952 cm^{-1}) observed in the latter sample after calcination is nearly the same as the (950 cm^{-1}) observed for the former sample in the dry state, the surface species formed after calcination in the sample with 2.5 wt% WO_3 is conjectured to have either an isolated tetrahedral or a relatively less-distorted octahedral structures. Invoking the XANES studies[23] that at coverages of less than 1/3 monolayer the surface tungsten species on γ-Al_2O_3 assumes an octahedral site symmetry, we favor at the moment the latter view, *i.e.* the octahedral stucture. In addition, it is interesting to observe that the phase transition from anatase to rutile has occurred to a greater extent when the sample with 2.5 wt% WO_3 was calcined at 973 K. When the calcination was performed at 823 K, such a phase change was hardly observable. Furthermore, for the samples with 6.2 or 10.2 wt% WO_3, we could not observe the phase transformation even after calcining at 973 K. Considering that substantial amount of phase transition occurs even at 770 K for TiO_2 itself, the surface tungsten species seems to retard the structural changes in TiO_2. This observation suggests that the interaction between tungsta and titania is, in fact, fairly strong. Nevertheless, the interaction looks to be active in the interfacial region since the WO_3 phase can be seen in the Raman spectra for the WO_3 /TiO_2 system in the calcined state as long as the tungsta loading exceeds the monolayer coverage. The presence of water vapor seems not to be enough to produce the surface tungsten species. Under the condition of multilayer coverage,

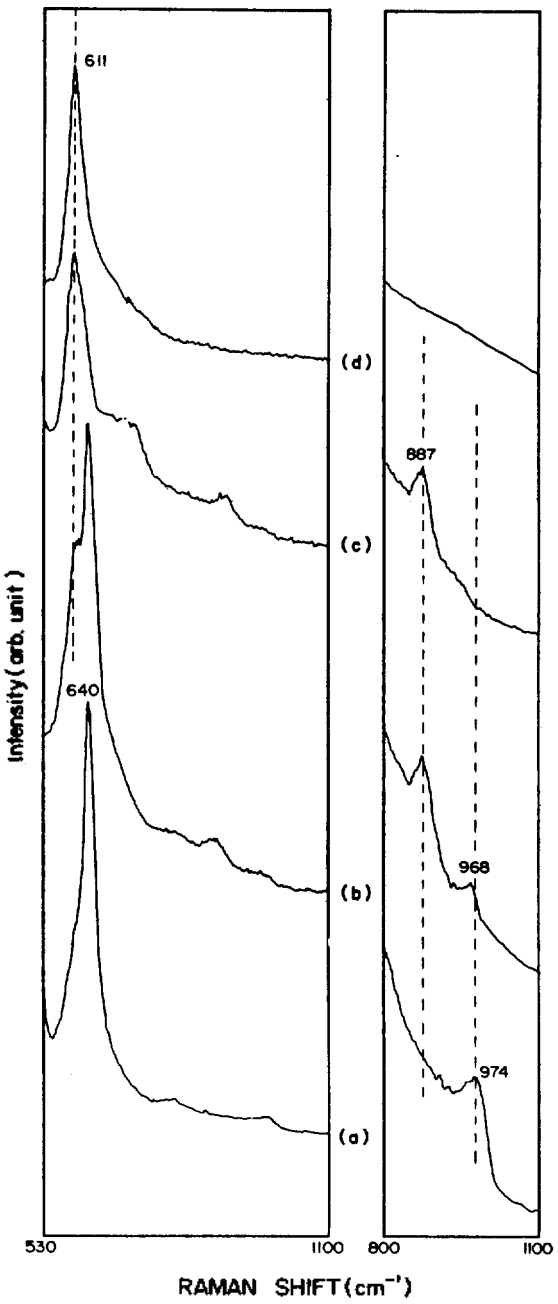

Figure 4. Raman spectra taken after calcining at 973 K for the samples of (a) 6.2 wt% WO_3 in TiO_2, (b) 1 wt% Ni plus 6.2 wt% WO_3 in TiO_2, (c) 3 wt% Ni plus 6.2 wt% WO_3 in TiO_2, and (d) TiO_2.

free surface hydroxyls of titania may not be available. Accordingly, it appears that surface hydroxyl group of TiO_2 is involved in the formation of surface polytungstate species.

The surface polytungstate species are observed to be very stable with respect to the repeated treatment of reduction under H_2 and subsequent calcination in air. As the calcined sample was treated with H_2 at 673 K, the sample became dark and any Raman spectral pattern attributable to tungsten species could not be observable. The Raman spectrum of the sample after recalcination at 823 or 973 K exhibited, however, the same characteristics as that observed prior to the reduction process. The spectral feature in the calcined

state is hardly dependent on the number of such a combined treatments.

In a separate experiment, we have investigated the spectral changes induced by the incorporation of additives, Ni and Co, to the tungsta catalysts. The typical Raman spectra for the samples containing 6.2 wt% WO_3 in TiO_2 after calcination at 973 K are shown in Figure 4. Figure 4a corresponds to a sample without any additive. On the other hand, Figure 4d is due to TiO_2 which has a rutile structure transformed from anatase by the thermal treatment at 973 K. As can be seen from Figure 4b, the band attributable to surface polytungstate shifted to a lower frequency with a somewhat decreased intensity as 1 wt% Ni was added to the sample, while a new peak centered at 887 cm ^{1} appeared. It can also be noticed that substantial amount of phase transition has occurred for the titania support from anatase to rutile. As the nickel content was increased to 3 wt%, any peak attributable to the surface polytungstate was hardly discernible. The phase transformation of titania is nearly complete. In addition, a shoulder peak apperared at near 707 cm^{-1}. The peak at 887 cm^{-1} in Figure 4b or 4c can be attributed to the W-O stretching vibration of $NiWO_4$ which has an octahedral WO_6 groups[23]. On the other hand, the shoulder peak at 707 cm^{-1} may be arisen from the formation of nickel oxide. Similar observations could also be made for the samples containing Co as an additive. That is, the formation of the corresponding tungstate and oxide salts, $CoWO_4$ and Co_3O_4, appeared to be favorable processes. When the tungsta loading was in the excess of monolayer coverge, the presence of WO_3 was observed to be drastically reduced upon the incorporation of Ni or Co. Above observations dictate that the additives, Co or Ni, react preferably with both the surface polytungstate and the crystalline WO_3 layers. This, in turn, weakens the interaction between the tungsten species and the titania such that the phase transition of the support material is likely to occur. Hence, the role of additives is supposed to affect not only the surface tungsten species but also the titania structures. These structural changes should induce the variation of the catalytic properties and characteristics of the composite system.

The dispersion of spreading of metal oxides on supports is one of the problems currently being investigated in the supported catalysts. Leyrer *et al*[33]. have recently reported that MoO_3 spreaded on the surface of TiO_2 in the absence and presence of H_2O vapor. Furthermore, a chemical transformation of MoO_3 into a surface polymolybdate was only observed after calcination in the presence of H_2O vapor. We have observed that a surface polymolybdate forms on the titania surface irrespective of the sample preparation method[19]. Both samples prepared by either the impregnation method or the physical mixing of MoO_3 and TiO_2 produced the same final products after calcination in air. In contrast, the calcined physical mixture of WO_3 and TiO_2 exhibited somewhat different features from the sample prepared initially by the impregnation wetness method. When a physical mixture containing 5 wt% WO_3 in TiO_2 was calcined at 673 K, any structural change of WO_3 could be hardly observed. After calcination at 973 K, a small amount of surface polytungstate that substantial amout of phase transition had occurred for the support from anatase to rutile. For the corresponding sample prepared from the impregnation method, neither the phase transition of TiO_2 nor the formation of WO_3 occurred after a similar thermal threatment. From these observations it appears that the formation of surface polytungstate species for the impregnated sample does not proceed mainly *via* the production of WO_3. By the low energy ion scattering spectroscopy (ISS), Leyrer *et al*[33]. measured the depth profiles for the physical mixture of WO_3 and γ-Al_2O_3 before and after heat treatment at 820 K. Although less pronounced than MoO_3/Al_2O_3 and MoO_3/TiO_2 systems, the spreading of WO_3 seemed to occur after calcination in both the dry and moist atmospheres. Considering that a crystalline WO_3 phase forms easily upon thermal treatment of ammonium paratungstate (the precursor used in the impregnation method), the titania support is, in fact, belived to interact strongly with the impregnation precursor during the calcination process. An intimate interfacial contact seems necessary to produce the surface polytungstate species. In order for the surface polytungstate species to form from WO_3 on TiO_2, the spreading of WO_3 on TiO_2 seems to be a prerequisite condition. Since the spreading of WO_3 on TiO_2 is too slow, the phase transition of titania should take place favorably as observed in this work.

In summary, we have applied Raman spectroscopy to the characterization of the tungsta catalyst supported on titania. The surface tungsten species which forms on titania after calcination appears to possess a structure that is independent of the initial impregnation condition. Although the identity of the surface species is a matter of conjecture, it seemed more or less to have a polytungstate structure with octrahedral site symmetry. The surface polytungstate looks stable in the interfacial region since the crystalline WO_3 phase is observed after calcination as far as the tungsta loading is in excess of monolayer coverage. The stability of the surface polytungstate could be evidenced further by the repeated treatment of reduction and subsequent calcination. Nevertheless, the incorporation of additives, Ni or Co, was found to suppress the existence of surface polytungstate species, producing the crystalline nickel (cobalt) tungstate. The spreading of WO_3 over the titania surface appeared to occur very slowly. Accordingly, the formation of surface polytungstate is supposed not to proceed *via* the formation of WO_3. The close intact and strong interaction between the polytungstate and the titania can be notified from the inhibition of the phase transition of TiO_2 from anatase to rutile.

Acknowledgement. This work was supported in part by the Korea Science and Engineering Foundation (890306-12).

References

1. P. Grange, *Catal. Rev. -Sci. Eng.*, **21**, 135 (1980).
2. F. E. Massoth and G. Muralidhar, *Proc. 4th Intern. Conf. on the Chemistry and Uses of Molybdenum*, Golden USA, 343 (1982).
3. J. R. Katzer and R. Sivasubramanian, *Catal. Rev. -Sci. Eng.*, **20**, 155 (1979).
4. J. Weitkamp, W. Gerhardt, and D. Scholl, *Proc. 8th Intern. Congr. on Catalysis*, Vol. II, 269, Dechema/Verlag Chemie, Weinheim (1984).
5. B. Vielhaber and H. Knözinger, *Appl. Catal.*, **26**, 375 (1986).

6. V. Kettmann, P. Balgavy, and L. Sokol, *J. Catal.*, **106**, 85 (1987).
7. A. Redy, J. Goldwasser, and W. K. Hall, *J. Catal.*, **113**, 82 (1988).
8. S. R. Seyedmonier and R. F. Howe, *J. Catal.*, **110**, 216 (1988).
9. M. D. Arco, A. Cahallero, P. Mallet, and V. Rivers, *J. Catal.*, **113**, 120 (1988).
10. K. Segawa, D. S. Kim, Y. Kurusu, and I. E. Wachs, *Proc. 9th Intern. Congr. on Catalysis, Vol. IV, 1960, Calgary* (1988).
11. S. J. Tauster, S. C. Fung, and R. L. Garten, *J. Am. Chem. Soc.*, **110**, 170 (1978).
12. S. J. Tauster and S. C. Fung, *J. Catal.*, **54**, 29 (1978).
13. R. T. K. Baker, S. J. Tauster, and J. A. Dumesic, Eds., *Strong Metal-Support Interactions*, American Chemical Sociey, Washington, DC (1986).
14. C. R. F. Lund and J. A. Dumesic, *J. Phys. Chem.*, **85**, 3175 (1981).
15. Y. I. Yermakov, B. N. Kuznetsov, and V. A. Zakharov, *Catalysis by Supported Complexes*, Elsevier, Amsterdam (1981).
16. S. Yuen, Y. Chen, J. E. Kubsh, and J. A. Dumesic, *J. Phys. Chem.*, **86**, 3022 (1982).
17. S. Soled, L. Murrell, I. Wachs, and G. McVicker, *Am. Chem. Soc. Div. Pet. Chem. Prepr.*, **28**, 1310 (1983).
18. K. Kim and S. B. Lee, *Bull. Kor. Chem. Soc.*, in Press.
19. H. S. Kim, S. H. Han, and K. Kim, Submitted for publication.
20. N. Kakuta, K. Tohji and Y. Udagawa, *J. Phys. Chem.*, **92**, 2583 (1988).
21. S. S. Chan, I. E. Wachs, L. L. Murrell, L. Wang, and W. K. Hall, *J. Phys. Chem.*, **88**, 5831 (1984).
22. I. E. Wachs and F. D. Hardcastle, *Proc. 9th Intern. Congr. on Catalysis, Vol. III, Calgary* 1440 (1988).
23. *J. A. Horsley, I. E. Wachs, J. M. Brown, G. H. Via, and F. D. Hardcastle, J. Phys. Chem.*, **91**, 4014 (1987).
24. I. R. Beattie and T. R. Gilson, *J. Chem. Soc.*, **A**, 2322 (1969).
25. K. Y. S. Ng and E. Gulari, Polyhedron **3**, 1001 (1984).
26. J. Aveston, *Inorg. Chem.*, **3**, 981 (1964).
27. N. Nakamoto, *Infrared and Raman Spectra of Inorganic and Coordination Compounds*, Wiley, New York (1978).
28. R. H. Busey and O. L. Keller, Jr., *J. Phys. Chem.*, **41**, 215 (1964).
29. J. P. Russell and R. Loudon, *Proc. Phys. Soc.*, **85**, 1029 (1965).
30. J. Hauck and A. Z. Fadini, *Naturforsch.* **B256**, 422 (1970).
31. F. Knee and R. A. Condrate, Sr., *J. Phys. Chem. Solids* **40**, 1145 (1979).
32. H. Jeziorowski and H. Knözinger, *J. Phys. Chem.*, **83**, 1166 (1979).
33. J. Leyrer, R. Margraf, E. Taglauer and H. Knözinger, *Surf. Sci.*, **201**, 603 (1988).

Synthesis and Biological Activity of Poly [(tri-O-acetyl-D-glucal)-*alt*-(maleic anhydride)] Derivatives

Man Jung Han*, Choong Whan Lee, Ki Ho Kim, and Won Young Lee†

Department of Applied Chemistry, Ajou University, Suwon 440-749
†Department of Microbiology, Yonsei University, Seoul 120-749. *Received September 17, 1990*

Poly[(tri-O-acetyl-D-glucal)-*alt*-(maleic anhydride)] was synthesized by free radical copolymerizations of the relevant comonomers. The alternating sequence of the copolymer was confirmed by ^{1}H-NMR, elemental analysis, and titration of anhydride groups incorporated into the copolymer. Hydrolysis of the copolymer under different conditions resulted in poly[(2-acetoxymethyl-3,4-diacetoxytetrahydropyran-5,6-diyl) (1,2-dicarboxyethylene)] and poly[(2-hydroxymethyl-3,4-dihydroxytetrahydropyran-5,6-diyl) (1,2-dicarboxyethylene)]. The cytotoxicities of these polymers measured against normal and tumor cells (3LL, B16) *in vitro* were found to be higher than that of DIVEMA, a prototype polymer having a high antitumor activity.

Introduction

It is well known that polymers with a high density of carboxylic acid functionality along the polymer chain can exhibit antitumor, antiviral and/or antifungal activities[1]. The tetrahydropyran (THP) rings as hydrophobic groups on the polymer chain may also play a significant role in the biological activity of the polymers[2]. We have synthesized several polymers containing THP rings and carboxyl groups on their backbone, which exhibit antitumor activity *in vitro* and *in vivo* comparable or superior to that of DIVEMA[3]. Among these polymers, poly[(2-acetoxytetrahydropyran-5,6-diyl) (1,2-dicarboxyethylene)] (1) and poly[(2-hydroxytetrahydropyran-5,6-diyl) (1,2-dicarboxyethylene)] (2) have been found to exhibit very high antitumor activities *in vitro* and *in vivo*[3,6].

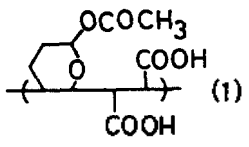

(1)

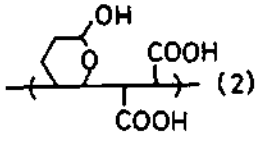

(2)